Inorganic Chemistry

Article

pubs.acs.org/IC

Photochemical Reactivity of the Iron(III) Complex of a Mixed-Donor, α-Hydroxy Acid-Containing Chelate and Its Biological Relevance to Photoactive Marine Siderophores

Jennifer E. Grabo, Mark A. Chrisman, Lindsay M. Webb, and Michael J. Baldwin*

Department of Chemistry, University of Cincinnati, P.O. Box 210172, Cincinnati, Ohio 45221-0172, United States

Supporting Information

ABSTRACT: The trimeric clusters $[Fe(III)_3(X\text{-}Sal\text{-}AHA)_3(\mu_3\text{-}OCH_3)]^-$, where X-Sal-AHA is a tetradentate chelate incorporating an α-hydroxy acid moiety (AHA) and a salicylidene moiety (X-Sal with X being 5-NO_2, 3,5-diCl, all-H, 3-OCH_3, or 3,5-di-*t*-Bu substituents on the phenolate ring), undergo a photochemical reaction resulting in reduction of two Fe(III) to Fe(II) for each AHA group that is oxidatively cleaved. However, photolysis of structurally analogous mixed Fe/Ga clusters demonstrate that a similar photolysis reaction will occur with only a single Fe(III) in the cluster. Quantum yields of iron reduction for the series of $[Fe(III)_3(X\text{-}Sal\text{-}AHA)_3(\mu_3\text{-}OCH_3)]^-$ complexes measured by monitoring Fe(II) production are twice those for ligand oxidation, measured by loss of the CD signal for the complex due to cleavage of the chiral AHA group. These moderate quantum yields, around 1−2% in the UVA and UVB range, are higher for complexes with electron-withdrawing X groups than for electron-donating X groups. The observed final photolysis product of the chelate is different if irradiation is done in the air than if it is done under Ar. The first observed photochemical product is the aldehyde resulting from decarboxylation of the AHA. This is the final product under anaerobic conditions. In air, this is followed by an Fe- and O_2-dependent reaction oxidizing the aldehyde to the corresponding carboxylate, then a second Fe- and light-dependent decarboxylation reaction giving a product that is two carbons smaller than the initial ligand. These reactivity studies have important biological implications for the photoactive marine siderophores. They suggest that different types of photochemical products for different siderophore structure types do not result from different initial photochemical steps, but rather from different susceptibility of the initial photochemical product to air oxidation.

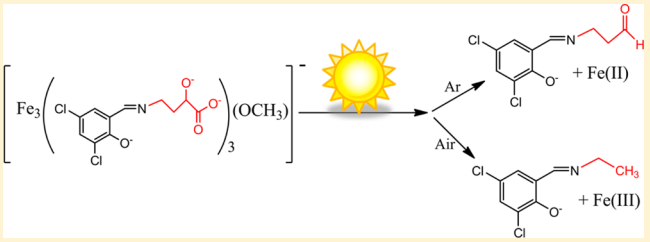

INTRODUCTION

In environments with limited Fe availability, including waters near the ocean surface, Fe acquisition can be growth limiting.[1,2] In order to sequester sufficient concentrations of bioavailable iron to sustain life, bacteria produce relatively low molecular weight biomolecules called siderophores that typically bind Fe(III) with high affinity.[3] The ferric stability constants (K_{ML}) for siderophores produced by bacteria in these marine environments range from as high as log K_{ML} = 51 for alterobactin,[4] through marinobactins and aquachelins with log K_{ML}'s in the mid-30s,[5] to as low as log K_{ML} = 24 for vibrioferrin.[6] Some of these marine siderophores undergo photochemical reactions that result in reduction of the Fe(III) to Fe(II) and oxidative cleavage of the siderophore. Butler and co-workers have shown through studies of numerous marine siderophores that those that are photochemically active include an α-hydroxy carboxylic acid (AHA) or closely related moiety among their Fe-coordinating functional groups.[3,7] The AHA moiety is reported to facilitate the photochemical reactivity of the Fe-bound siderophore through a near-UV ligand-to-metal charge transfer transition.[8,9]

Inspired by the photoactive marine siderophores, we have developed new AHA-containing chelates that are designed to tightly bind Fe(III) or other transition metals and to reduce and release the metal upon irradiation.[10] These chelates are not as structurally complex as the natural product marine siderophores. However, they have more structural variability and synthetic tunability of their transition metal coordination chemistry than other small natural AHAs, such as citrate and tartrate, which incorporate only other carboxylates among their metal-binding functional groups. Among these new AHA-containing chelates is a series of tetradentate ligands that incorporate a salicylidene moiety in addition to the AHA. These chelates have been designated X-Sal-AHA, where X is 5-NO_2, 3,5-diCl, all-H, 3-OCH_3, or 3,5-di-*t*-Bu as substituents on the phenolate ring. Each of these derivatives produces an Fe(III) cluster with the same trinuclear structure displayed by the crystal structure of $[Fe_3(3,5\text{-}diCl\text{-}Sal\text{-}AHA)_3(\mu_3\text{-}OCH_3)]^-$ (Scheme 1).[10] These clusters have especially high Fe(III) stability constants, but release Fe(II) to bidentate receptor ligands such as phenanthroline upon irradiation.

The AHA-containing chelates provide an alternative approach to the photoactive chelates referred to as photocages.[11] These photocages frequently take advantage of the photoactivity of a nitrophenyl group appended to the

Received: March 19, 2014
Published: May 19, 2014

   dx.doi.org/10.1021/ic500635q | Inorg. Chem. 2014, 53, 5781−5787

Scheme 1. Line Drawing of the General Structure of the Trinuclear Clusters $[Fe_3(X\text{-Sal-AHA})_3(\mu_3\text{-}OCH_3)]^{-}$ [10] [a]

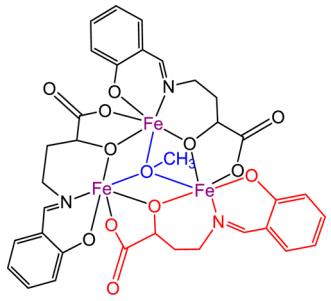

[a]The phenolate ring substituents, X, are not included.

chelate. Irradiation either reduces the metal binding ability of one or more coordinating groups[12] or fragments the chelate.[13−15] This approach was initially used with Ca(II) to examine its biological roles.[14,16] More recently it has been applied to other metals, including the biologically important d-block metals Cu(II),[13] Zn(II),[15] and Fe(III).[12] In contrast to the AHA-containing chelates, the photocages are photochemically sensitive in the absence of bound metal. In some cases, the quantum yield decreases upon metal binding.[13] The stability constants for metal binding by the photocages also tend to be rather moderate. The photocage FerriCast, for example, is highly selective for Fe(III) binding in nonaqueous solvents, but decomplexation occurs in solvents with oxygen donors such as water or alcohols.[12]

Due to the importance of the irradiation products in a number of potential applications that would employ tight metal binding with light-triggered metal release, we set out to thoroughly understand the light-initiated reactivity of the Fe(III) complexes of the X-Sal-AHA chelates. These chelates undergo photochemical reactions only when an appropriate metal, such as Fe(III), is bound. This differs from the photocages described above, but is similar to the AHA-containing marine siderophores. The presence of oxygen significantly affects the observed products after irradiation. Careful study of the step-by-step reactions that follow irradiation of the structurally characterized $[Fe(III)_3(3,5\text{-diCl-Sal-AHA})_3(OCH_3)]^{-}$ cluster was therefore undertaken under both aerobic and anaerobic conditions. Irradiation of the Ga(III) and mixed Fe(III)/Ga(III) clusters was also examined for comparison.

The results of these studies may have significant implications for interpreting the observed photochemical products of the natural marine siderophores. Different marine siderophores produce different kinds of photoproducts, which appear to correlate with specific structural features.[3] Many of the photoactive marine siderophores incorporate the α-hydroxy acid group through either a citrate-like moiety in the chelate backbone or a β-hydroxyaspartate group. Additionally, some marine siderophores make up suites of amphiphiles that vary based only on the characteristics of an appended fatty acid group, while others lack the fatty acid and are better described as hydrophilic. Both the citrate-based class of marine siderophores and the β-hydroxyaspartate-based class include examples of both amphiphilic and hydrophilic members. The citrate-based siderophores undergo a simple decarboxylation upon irradiation of the Fe(III) complex. Tautomerization of the ketone product to the enolate form results in little decrease in the Fe(III) stability constant compared to the intact siderophore. Petrobactin[8] and aerobactin[17] are hydrophilic examples of the citrate-based siderophores that result in this kind of product upon irradiation, and the ochrobactins[18] and synechobactins[19] are examples of amphiphilic siderophores within this class. Irradiation of the β-hydroxyaspartate-based siderophores results in more extensive cleavage. Amphiphilic examples such as the aquachelins[9] lose the fatty acid group upon irradiation. The alterobactins[4] are examples of hydrophilic, β-hydroxyaspartate-based siderophores. The Fe(III) stability constants of this class of siderophores tend to decrease more upon photolysis than do those of the citrate-based siderophores.[3]

Why marine bacteria have evolved to produce siderophores with these different structural properties remains an important question. Whether the fatty acid moiety is lost and whether there is a significant decrease in the strength of iron binding upon irradiation are certain to have significant functional consequences for the siderophores. A better understanding of the chemistry that leads to those differences will aid in answering that question. The results of studies presented here on the photochemistry of $[Fe(III)_3(3,5\text{-diCl-Sal-AHA})_3(OCH_3)]^{-}$ will contribute to interpreting the photochemistry of the marine siderophores.

EXPERIMENTAL SECTION

General Considerations and Synthesis. All solvents and chemicals were used as received from Fisher/Acros unless otherwise noted. Anaerobic samples were prepared in an MBraun LabStar glovebox with an Ar atmosphere and $[O_2] < 0.1$ ppm. The X-Sal-AHA chelates and their Fe complexes were prepared as described previously.[10] Additional purification to remove salts and any other impurities was accomplished by suspending the complex in a mixture of hexane and dibromoethane that matched the density of the complex, so that any impurities either sank or floated to the surface of the solution. Solutions of mixed Fe−Ga complexes were prepared by combining a methanolic solution containing $Fe(NO_3)_3{\cdot}9H_2O$ and $Ga(NO_3)_3$ with another methanolic solution containing one equivalent of 3,5-diCl-Sal-AHA and two equivalents of $KHCO_3$ per equivalent of total metal and stirring overnight. *N*-(3,5-Dichlorosalicylidene-β-alanine) (L′) was prepared by the Schiff base condensation of 3,5-dichlorosalicylaldehyde with β-alanine. Synthetic details for preparations of L′ and its Fe complexes and their characterization and of the mixed metal clusters of L are available in the Supporting Information.

Instrumental Methods. UV/visible absorption spectra were obtained using a Spectral Instruments, Inc. model 420 spectrophotometer, using either a fiber optic dip probe with a 1 cm path length or a cuvette accessory with a 1 cm quartz cuvette. For anaerobic measurements, samples were loaded into an anaerobic cuvette under an Ar atmosphere in the glovebox. Circular dichroism spectra were obtained on a Jasco J-715 spectropolarimeter. The CD intensity was converted from mdeg to molar absorptivity difference ($\Delta\varepsilon$) using $\Delta\varepsilon = \theta/32980[M]$ where θ is the ellipticity in mdeg and [M] is the molar concentration of the analyte. Electrospray ionization mass spectrometry (ESI-MS) data were collected at the University of Cincinnati Mass Spectrometry Facility on a Micromass Q-TOF-2 spectrometer.

Photochemical Experiments. Irradiation of samples was accomplished using a Luzchem LZC 4 V photoreactor with sets of 16 lamps provided by Luzchem Research, Inc. (Ottowa, Ontario, Canada) centered at 300 nm (UVB), 350 nm (UVA), or 420 nm (LZC-420). Samples were in 2.5 dram type I, class B borosilicate glass vials on a rotating, merry-go-round-type sample holder. Lamp intensity was calibrated using 0.6 mM solutions of $K_3[Fe(oxalate)_3]$, prepared as described in the literature, as the actinometer.[20] The intensity was calculated using the following formula: $I = [Fe^{2+}] \times N_A/(\Phi_\lambda \times \Delta t)$ where N_A is Avogadro's number, Φ_λ is the quantum yield of $K_3[Fe(oxalate)_3]$ in the wavelength range of interest, and Δt is time at 1, 3, 7, 15, and 30 s. $[Fe^{2+}]$ in the irradiated sample was found by

dx.doi.org/10.1021/ic500635q | Inorg. Chem. 2014, 53, 5781−5787

adding 2.0 mL of 0.1% *o*-phenanthroline solution and 2.0 mL of sodium acetate buffer to 4.0 mL of the actinometer solution, then diluting the solution to 20 mL and measuring the absorbance of $[Fe(phen)_3]^{+2}$ at 510 nm (ε = 11 100 M^{-1} cm^{-1}). Quantum yields were determined by monitoring either Fe reduction or ligand cleavage at various time points by which photolysis was no more than one-third complete. The reported values are the average of two separate time points within the linear part of the time course from each of three independent trials. The reported error values are the standard deviation for these six measurements. The concentration of the Fe complex was 0.3 mM during irradiation with absorbance across the wavelength range of interest greater than 1, so that >90% of photons impinging on the sample were absorbed. Iron reduction was monitored by determining the concentration of $Fe(II)(BPDS)_3^{4-}$ in solutions that were diluted to 0.04 mM in the presence of excess BPDS (bathophenanthroline disulfonate). The $Fe(II)(BPDS)_3^{4-}$ complex absorbs intensely with a maximum at 535 nm, while there is little absorbance in the visible range for Fe(III) solutions with BPDS. The reported values are from experiments done anaerobically to prevent any air oxidation of the reduced iron. The molar absorptivity of $Fe(II)(BPDS)_3^{4-}$ has been reported over a range varying by more than 10%,[9,21] so the value used for the calculations reported here was determined independently in this lab as ε = 20 500 M^{-1} cm^{-1} in methanol, which is in the middle of the range of literature values. The quantum yield of Fe reduction was calculated using the equation $\Phi_{Fe} = [Fe^{2+}] \times N_A/(I \times \Delta t)$. Ligand cleavage was monitored using circular dichroism spectroscopy. The α-carbon of the α-hydroxy acid group is chiral, providing a CD signal for the intact complex. Loss of the chiral center upon cleavage is monitored as a decrease in the CD intensity. This experiment is done under aerobic conditions, to allow air oxidation of the reduced Fe so that the intact ligand will re-form the cluster and provide CD intensity that accurately corresponds to the amount of remaining ligand. The quantum yield for ligand cleavage was calculated from the following equation: $\Phi_L = [L] \times N_A/(I \times \Delta t)$ where [L] is the decrease in concentration of chiral ligand during irradiation.

RESULTS

Metal:Chelate Ratios in Photolysis Reaction. Upon irradiation of $[Fe_3(3,5\text{-diCl-Sal-AHA})_3(OCH_3)]^-$ with ultraviolet light, the Fe(III) is reduced to Fe(II), and the 3,5-diCl-Sal-AHA^{3-} chelate is cleaved. (The nature of this cleavage is addressed below.) This photolysis reaction can be monitored from the point of view of either the iron reduction or the chelate cleavage. Production of Fe(II) can be monitored spectrophotometrically by addition of the phenanthroline derivative BPDS, which shows an intense visible absorption when coordinated to Fe(II) as $Fe(BPDS)_3^{4-}$. The α-carbon of the AHA group in the 3,5-diCl-Sal-AHA^{3-} chelate is chiral, so it shows a strong circular dichroism (CD) signal whether it is free or coordinated to a metal. The photolysis reaction results in loss of the chiral center, so the chelate cleavage can be monitored by loss of the CD signal. Under aerobic conditions, the CD signal disappears entirely after sufficient irradiation to drive the photolysis reaction to completion, and a majority of the iron (around 70%) is detected as Fe(II) based on the absorbance at 535 nm when BPDS is present.[10] Under anaerobic conditions, however, while nearly all of the iron is detected as Fe(II), some CD signal remains, indicating that some of the chelate remains intact even after extensive irradiation.

The ratio of Fe reduction to chelate cleavage was determined for anaerobic irradiation of $[Fe_3(3,5\text{-diCl-Sal-AHA})_3(OCH_3)]^-$, so that reoxidation of Fe(II) by air is not available to drive chelate photolysis beyond the single photolysis event ratio. As indicated above, after 60 min of irradiation under UVA light in the presence of BPDS, >90% of the Fe is detected as Fe(II) based on the intensity of the 535 nm feature in the UV/visible absorption spectrum. After the same amount of time, some CD intensity remains, as shown in Figure 1. This CD signal is very

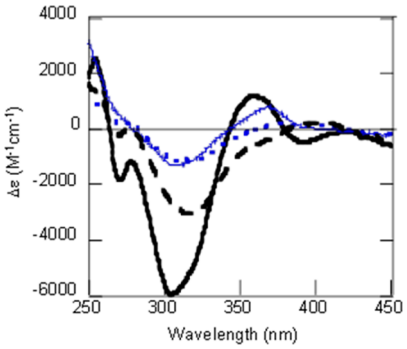

Figure 1. Circular dichroism spectra of 0.0375 mM methanolic solutions of $Na[Fe_3(3,5\text{-diCl-Sal-AHA})_3(OCH_3)]$ before irradiation (thick black solid line), after irradiation under Ar (blue dotted line), after irradiation under Ar, and then on exposure to air (black dashed line), and a solution of a 1:1 mixture of Fe(II) and 3,5-diCl-Sal-AHA (thin blue solid line).

similar to the CD of a solution of the 3,5-diCl-Sal-AHA chelate prepared with one equivalent of $Fe(II)(NO_3)_2$. In order to determine the percentage of intact chelate represented by this CD signal, the sample (without BPDS) was opened to the air in the dark to allow the iron to air oxidize to Fe(III) under nonphotolyzing conditions. This should result in reassembly of the $[Fe_3(3,5\text{-diCl-Sal-AHA})_3(OCH_3)]^-$ cluster from any remaining intact Sal-AHA chelate so that the CD signal intensity can be directly compared to that of the initial solution prior to irradiation. The CD spectrum in the presence of Fe(III) corresponds to 53% of the chelate remaining intact after irradiation, based on three independent measurements, or 47% cleavage of the chelate. These data are consistent with a 2:1 ratio of iron reduction to chelate cleavage in the anaerobic photolysis reaction.

While the 2:1 ratio determined above is consistent with that observed for the Fe(III)-citrate complex,[22] which has been shown to be a $Fe_2(cit)_2$ dimer,[23] the ratio is assumed to be 1:1 for the marine siderophores that bind a single iron. In order to determine whether the photochemical reaction would still occur with only a single Fe(III) in the complex, irradiation of a solution that includes mixed-metal Fe/Ga complexes of 3,5-diCl-Sal-AHA with the same trimeric structure as $[Fe_3(3,5\text{-diCl-Sal-AHA})_3(OCH_3)]^-$, was examined. The Ga(III) complex of 3,5-diCl-Sal-AHA^{3-} has been structurally characterized.[24] It has a very similar structure to $[Fe_3(3,5\text{-diCl-Sal-AHA})_3(OCH_3)]^-$, but it is not photoactive, as expected. When Ga(III) and Fe(III) are together combined with 3,5-diCl-Sal-AHA^{3-}, a mixture that includes the all-Fe and all-Ga trimers, as well as the 2:1 Fe:Ga and 1:2 Fe:Ga mixed-metal trimers, is produced.[24] This facilitates an experiment to determine whether two Fe(III) ions are *required* in the cluster for the photolysis reaction to occur. The main features in the ESI mass spectrum of the solution resulting from combination of Fe(III), Ga(III), and 3,5-diCl-Sal-AHA^{3-} are centered near m/z of 1065, 1079, 1093, and 1107. These features correspond to the Fe_3, Fe_2Ga, $FeGa_2$, and Ga_3 clusters, respectively. Upon irradiation for 30 min under either aerobic or anaerobic conditions, all three of the Fe-containing peaks disappear, leaving only the Ga_3 cluster, as

dx.doi.org/10.1021/ic500635q | Inorg. Chem. 2014, 53, 5781−5787

shown in Figure 2. After shorter periods of irradiation, the rate of disappearance of all three Fe-containing clusters appears to be similar (Figure S6).

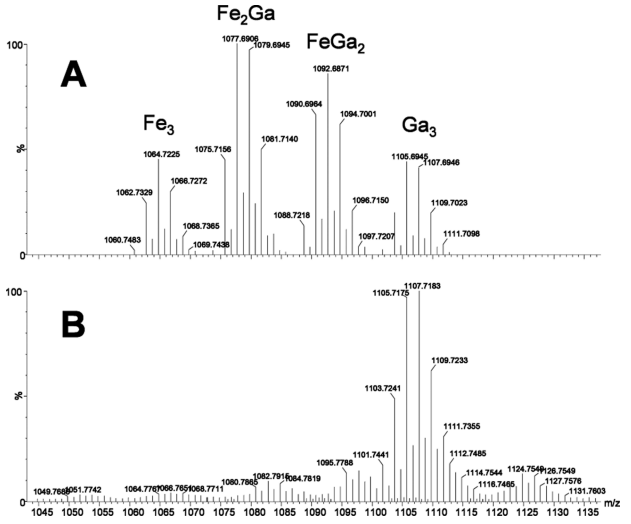

Figure 2. ESI mass spectrum of Fe(III):Ga:(3,5-diCl-Sal-AHA) 1:2:3 in methanol (A) before irradiation and (B) after irradiation with UVA light. The 1:2 ratio of Fe:Ga was used to compensate for the greater sensitivity of the mass spectrometer to the Fe complexes; however the same result is observed for the 1:1:2 ratio of Fe:Ga:L (see Figure S5).

Quantum Yields for $[Fe_3(X\text{-}Sal\text{-}AHA)_3(OCH_3)]^-$. The quantum yields for photolysis of the $[Fe_3(X\text{-}Sal\text{-}AHA)_3(OCH_3)]^-$ complexes can be determined based on either iron reduction or chelate cleavage. The quantum yield for anaerobic iron reduction (Φ_{Fe}) is based on determination of Fe(II) concentration through the spectrophotometric assay with BPDS described above and shown in Figure 3. The value

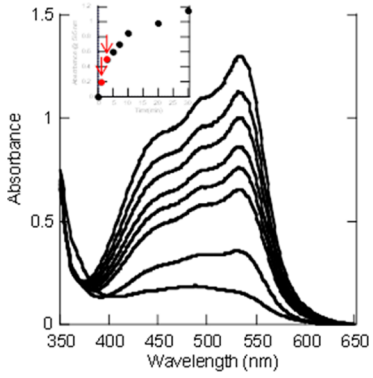

Figure 3. UV/vis absorbance spectra of $Na[Fe_3(3,5\text{-diCl-Sal-AHA})_3(OCH_3)]$ (0.0375 mM in methanol) in the presence of excess BPDS after irradiation with UVA light for 0, 1, 3, 5, 7, 10, 20, and 30 min (absorbance increasing with time). Inset: Absorbance at 535 nm, with the points used to calculate quantum yields indicated by red arrows.

of Φ_{Fe} is calculated to be somewhat lower when determined under air presumably due to some competition between air oxidation of the Fe(II) to Fe(III) and its formation of $Fe(II)(BPDS)_3^{4-}$. The quantum yield for ligand cleavage (Φ_L) is based on decrease in the concentration of the intact AHA ligand determined by loss of the CD signal. The Fe reduction to ligand cleavage stoichiometry determined above indicates that the quantum yield of a single photochemical event upon irradiation, Φ, should correspond to reduction of two Fe(III) with cleavage of one chelate, or $\Phi = \Phi_L = {}^1/_2\Phi_{Fe}$. The quantum yields determined by each method are reported in Table 1 for Fe(III) complexes of four different phenyl ring-substituted derivatives of Sal-AHA.

Photolysis Products of $[Fe_3(3,5\text{-diCl-Sal-AHA})_3(OCH_3)]^-$. Irradiation of a methanolic solution of $Na[Fe_3(3,5\text{-diCl-Sal-AHA})_3(OCH_3)]$ by near-UV light under anaerobic conditions for 60 min results in loss of the feature corresponding to the monoanionic, trimeric cluster at m/z = 1065 in the ESI-MS experiment (Figure S1), with a feature at m/z = 244 growing in (Figure S7). This new feature corresponds to a loss of 44 mass units from the intact $[3,5\text{-diCl-Sal-AHA}]^{3-}$ chelate, along with loss of the strong Fe binding. This is consistent with decarboxylation of the AHA moiety to produce an aldehyde with one fewer carbon atom. Additional irradiation of this solution under anaerobic conditions does not result in further changes. In order to test whether this product acts like an aldehyde, propylamine was added to the solution of the photolysis product. This resulted in new features in the ESI-MS at m/z = 114 and 232 (Figure S8). The m/z = 114 feature corresponds to the Schiff base that would be formed by reaction of propylamine with 3-aminopropionaldehyde, while the m/z = 232 feature corresponds to the Schiff base of propylamine with 3,5-diCl-salicylaldehyde.

Irradiation by near-UV light of a methanolic solution of $Na[Fe_3(3,5\text{-diCl-Sal-AHA})_3(OCH_3)]$ prepared in the same way but under air results not in the aldehyde but rather in a different product. The main product observed by ESI-MS under these conditions occurs at m/z = 216 (Figure S9) and corresponds to loss of 72 mass units from 3,5-diCl-Sal-AHA or a further 28 mass units from the aldehyde product of anaerobic irradiation. A series of experiments was undertaken to determine the conditions under which irradiation resulted in the aldehyde versus the more extensive chelate cleavage. Conditions included presence or absence of air, as well as exposure to air after anaerobic irradiation. The results of these experiments, monitored by ESI-MS, are listed in Table 2. Under conditions that prevent air oxidation of Fe(II), the major product is the aldehyde at m/z = 244. As noted above, the major product due to photolysis under air is at m/z = 216, corresponding to a net loss of CO from the aldehyde. When $Na[Fe_3(3,5\text{-diCl-Sal-AHA})_3(OCH_3)]$ is irradiated under anaerobic conditions, and the product is then exposed to air in the dark, different products appear at m/z = 576 and 732 (Figure S10). These features correspond to Fe complexes that include the carboxylate (designated L′) resulting from air oxidation of the aldehyde product of anaerobic irradiation. During irradiation under air in the presence of phenanthroline, which partially protects Fe(II) from air oxidation back to Fe(III), oxidation of the aldehyde is slowed substantially (Figure S11), with a significant amount of aldehyde remaining after 2 h of aerobic irradiation. Taken together, these data suggest the reaction sequence shown in Scheme 2.

In order to test this proposed reaction scheme, the compound with an m/z of 260, L′ = *N*-(3,5-dichlorosalicylidene-*β*-alanine), was synthesized. While crystal structures of this ligand with several different metals have been reported,[25,26] the structure of the Fe complex has not. When L′ is added to Fe(III), this produces the complex $Fe(III)L'_2$, with a feature at m/z = 576 in the ESI-MS experiment (Figure S4). This corresponds to the feature observed in the mass spectrum of

dx.doi.org/10.1021/ic500635q | Inorg. Chem. 2014, 53, 5781−5787

Table 1. Quantum Yields for Irradiation of the $[Fe_3(X\text{-Sal-AHA})_3(\mu_3\text{-}OCH_3)]^-$ Complexes with Different Wavelength Ranges[a]

	UVB			UVA			LZC-420		
X	Φ_{Fe}	Φ_L	Φ	Φ_{Fe}	Φ_L	Φ	Φ_{Fe}	Φ_L	Φ
5-NO_2	4.3 ± 0.1	1.3 ± 0.7	1.7	4.2 ± 0.1	1.5 ± 0.1	1.8	2.2 ± 0.1	0.8 ± 0.2	0.9
3,5-diCl	2.4 ± 0.3	1.3 ± 0.2	1.2	2.6 ± 0.3	1.0 ± 0.2	1.1	0.8 ± 0.1	0.3 ± 0.1	0.4
all-H	1.0 ± 0.3	0.7 ± 0.1	0.6	0.9 ± 0.2	0.6 ± 0.1	0.5	0.6 ± 0.2	0.2 ± 0.1	0.3
3-OCH_3	1.6 ± 0.1	0.7 ± 0.1	0.7	1.4 ± 0.2	0.8 ± 0.2	0.8	0.7 ± 0.1	0.2 ± 0.1	0.3

[a]Φ is the average of the values for Φ_L and $^1/_2\Phi_{Fe}$, given in % yield.

Table 2. Species Observed by ESI-MS under Different Conditions Due to Irradiation by UVA

m/z	dark air or Ar	UVA Ar	UVA air	UVA Air + phen	UVA Ar, then dark air
1065	×				
244		×		×	
216			×	×	
576					×

Scheme 2. Reaction Sequence for $Na[Fe_3(3,5\text{-diCl-Sal-AHA})_3(OCH_3)]$ Following Irradiation

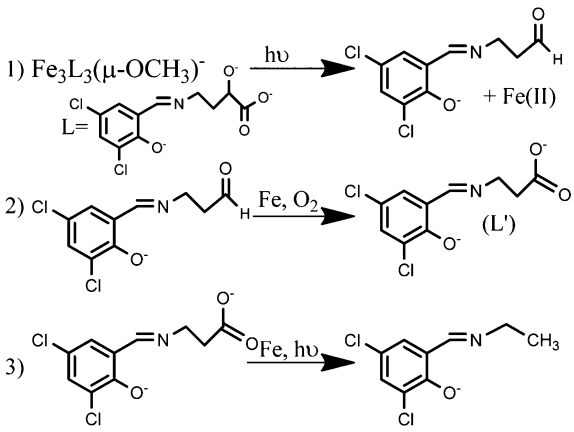

the product of reaction 2 in Scheme 2. Irradiation of this complex results in a product with *m/z* = 216 (Figure S12), identical to the final product observed after irradiation of $Na[Fe_3(3,5\text{-diCl-Sal-AHA})_3(OCH_3)]$ in the air. In contrast, irradiation of L′ under Ar in the presence of Fe(II) does not produce the feature at *m/z* = 216 (Figure S13).

DISCUSSION

The X-Sal-AHA series of chelates that incorporate a salicylidene moiety and an α-hydroxy acid moiety, with variable electron-donating or -withdrawing groups on the phenolate ring, was reported to form trimeric clusters with Fe(III) in the form $[Fe_3(X\text{-Sal-AHA})_3(\mu_3\text{-}OCH_3)]^-$.[10] These clusters were shown to be photoactive in sunlight, with the resulting photochemical reaction substantially decreasing the high stability constants of the initial trimers, allowing preferential binding of the resulting Fe(II) by a phenanthroline derivative. This irreversible photochemical reaction was shown to result from the interaction between the Fe(III) and the chelate, as there was no observable change in the free chelate when irradiated by sunlight. In this paper, details of that photochemical reaction of the Fe(III) cluster complex are reported. The results of these studies have important implications for the photochemical reactions of the marine siderophores that inspired the X-Sal-AHA chelates, as discussed below.

Comparison of the amount of Fe(II) produced and chelate cleavage incurred upon anaerobic irradiation, as monitored by the spectrophotometric detection of the resulting Fe(II)-$(BPDS)_3$ complex, and the loss of the chiral center in the AHA moiety monitored by the decrease in the CD signal, respectively, demonstrates a 2:1 metal reduction to chelate decarboxylation ratio. This is consistent with the ratio suggested previously,[10] based on the residual CD intensity observed upon extensive irradiation only under anaerobic conditions, and also the reported photochemical reaction of $Fe(III)_2(citrate)_2$.[22] This ratio is consistent with the pair of one-electron reductions of Fe(III) to Fe(II) corresponding to a single two-electron oxidative decarboxylation of the AHA moiety to give the aldehyde.

If the 2:1 ratio of Fe reduction to chelate cleavage were the result of a *requirement* for two reducible irons in the complex in order to result in photochemically induced oxidative decarboxylation of the AHA, then a cluster with only one Fe(III) would not be expected to undergo photolysis. This is contrary to the observation for the mixed FeGa clusters, in which not only the Fe_2Ga cluster but also the $FeGa_2$ cluster is photoactive. While the all-Ga cluster is photochemically inert, this experiment shows that only a single Fe(III) is required for the photochemical reaction to occur. These apparently contradictory observations are rectified by considering results of laser flash photolysis studies by Glebov at al. of other related Fe(III)-carboxylate complexes. Those studies, under conditions in which only a single Fe(III) is coordinated to the activated carboxylates, were interpreted as indicating that "...[the photolysis] mechanism is based on the formation of a long-lived complex between Fe(II) and organic radical".[27] In the presence of a second Fe(III), this Fe(II)-radical complex would be further oxidized by one electron, resulting in the observed two Fe(II) ions and the two-electron-oxidized decarboxylation product. In the case of the α-hydroxy acids, that product would be the aldehyde. In the absence of the second Fe(III), as in the $FeGa_2$ cluster, or the marine siderophores, the second electron would go to any available site that would lower the overall energy, including perhaps solvent.

Quantum yields for the photolysis of several members of the $[Fe(III)_3(X\text{-Sal-AHA})_3(\mu\text{-}OCH_3)]^-$ series were determined by monitoring both the Fe(II) production and the loss of the chiral center on the AHA group. Quantum yields based on the amount of Fe(II) produced (Φ_{Fe}) are about twice those based on the amount of loss of the AHA chiral center (Φ_L). This 2:1 ratio of Φ_{Fe}:Φ_L determined after brief exposure to light further supports the ratio determined by measuring the amount of Fe(II) produced and intact AHA remaining after exhaustive photolysis as described above. The trend in the quantum yields in each of the wavelength ranges examined agrees with the relative rates of photolysis observed previously under sunlight.[10] That is, more electron-withdrawing ring substituents on the phenolate of the X-Sal-AHA chelate result in higher

dx.doi.org/10.1021/ic500635q | Inorg. Chem. 2014, 53, 5781−5787

quantum yields. In the UVA and UVB wavelength ranges, the quantum yields for the different complexes are in the range $\Phi = \Phi_L = {}^1/_2\Phi_{Fe} = 0.5-2\%$.

Although exhaustive photolysis of $Na[Fe_3(3,5\text{-diCl-Sal-AHA})_3(OCH_3)]$ appears to produce different products depending on the presence or absence of air, the reaction under either condition proceeds through decarboxylation of the AHA moiety to produce an aldehyde. This step of the sequence of reactions in Scheme 2 is likely initiated by a ligand-to-Fe(III) charge transfer that is consistent with the excited state observed for other Fe-carboxylate complexes in earlier laser flash photolysis experiments.[27] An electron transfer from the radical produced by the initial photochemical event to a second Fe(III) in the cluster results in oxidative release of CO_2 to form the aldehyde. In the absence of air, no further reaction takes place and the aldehyde is the final observed product. The addition of propylamine confirms the chemical nature of the aldehyde. Although the Schiff base corresponding to reaction of propylamine with the aldehyde product shown in reaction 1 of Scheme 2 is not observed, two products consistent with displacement of 3-aminopropionaldehyde from the salicylidene linkage by propylamine are observed. One is the Schiff base resulting from reaction of propylamine with the salicylidene fragment, and the other is the Schiff base resulting from reaction of propylamine with the 3-aminopropionaldehyde fragment. This latter species demonstrates the aldehyde nature of the photolysis product.

When the anaerobic product of photolysis, including the aldehyde and Fe(II), are exposed to air without further irradiation, the carboxylate product of reaction 2 in Scheme 2 (designated L′) is produced. When phenanthroline is present to protect the Fe(II) from air oxidation to Fe(III), much less oxidation of the aldehyde product occurs. Together, these observations show that the aldehyde oxidation step is dependent on both O_2 and iron, but is not light driven. The final step to give the product of reaction 3 in Scheme 2 is light driven, as the reaction stops at the carboxylate in the absence of further irradiation. It is also dependent on Fe(III), as the synthetic L′ does not undergo photolysis in the absence of iron or in the presence of only Fe(II).

The comparison of aerobic and anaerobic photolysis products of $Na[Fe_3(3,5\text{-diCl-Sal-AHA})_3(OCH_3)]$ has important implications for the differences observed for marine siderophores with different AHA frameworks. Those based on a citrate backbone are reported to undergo simple decarboxylation, while the β-hydroxyaspartate-based siderophores undergo much more extensive cleavage.[8,9] The studies reported here suggest that this apparently large difference in reactivity is not due to differences in the initial photochemical and chemical steps. Rather, the difference is likely due to differences in susceptibility of the decarboxylation product to air oxidation in the presence of iron. Decarboxylation of the citrate moiety produces a ketone, which is resistant to air oxidation. However, decarboxylation of the β-hydroxyaspartate moiety produces an aldehyde, which, in the presence of iron and oxygen, is oxidized to a carboxylate, which can undergo further photolysis when coordinated to Fe(III). In many of the amphiphilic marine siderophores, the characteristic fatty acid group is attached near the photolysis site and is cleaved from the main body of the molecule when the additional photolysis reactions occur. If the β-hydroxyaspartate-based marine siderophores were irradiated under anaerobic conditions, this would predict that simple decarboxylation of the AHA group to the aldehyde would be observed; however, the reported studies on photolysis of marine siderophores all appear to have been conducted in air. The data reported here provide significant insight into the chemical basis for the difference in photolysis products for the citrate-based and β-hydroxyaspartate-based marine siderophores. The question as to why some marine bacteria evolved to produce siderophores that give an oxygen-sensitive photolysis product that results in cleavage of the fatty acid moiety, while others evolved to produce siderophores that are resistant to this cleavage, remains an interesting question.

■ ASSOCIATED CONTENT

Ⓢ Supporting Information

Details of the synthesis and characterization of *N*-salicylidene-β-alanine and its Fe(III) complex, details of the preparation of the mixed Fe/Ga clusters, and Figures S1−S13 including all mass spectra referred to in the text. This material is available free of charge via the Internet at http://pubs.acs.org.

■ AUTHOR INFORMATION

Corresponding Author

*E-mail: Michael.baldwin@uc.edu.

Notes

The authors declare no competing financial interest.

■ ACKNOWLEDGMENTS

This research was supported by NSF grant CHE-0955603. The authors thank Prof. Apryll Stalcup for the use of the circular dichroism spectrophotometer.

■ REFERENCES

(1) Martin, J. H.; Coale, K. H.; Johnson, K. S.; Fitzwater, S. E.; Gordon, R. M.; Tanner, S. J.; Hunter, C. N.; Elrod, V. A.; Nowicki, J. L.; Coley, T. L.; Barber, R. T.; Lindley, S.; Watson, A. J.; VanScoy, K.; Law, C. S.; Liddicoat, M. I.; Ling, R.; Stanton, T.; Stockel, J.; COllins, C.; Anderson, A.; Bidigare, R.; Ondrusek, M.; Latasa, M.; Millero, F. J.; Lee, K.; Yao, W.; Zhang, J. Z.; Friederich, G.; Sakamoto, C.; Chavez, F.; Buck, K.; Kolber, Z.; Greene, R.; Falkowski, P.; Chisholm, S. W.; Hoge, F.; Swift, R.; Yngel, J.; Turner, S.; Nightingale, P.; Hatton, A.; Liss, P.; Tindale, N. W. *Nature* **1994**, *371*, 123−129.

(2) Bruland, K. W.; Donat, J. R.; Hutchins, D. A. *Limnol. Oceanogr.* **1991**, *36*, 1555−1577.

(3) Butler, A.; Theisen, R. M. *Coord. Chem. Rev.* **2010**, *254*, 288−296.

(4) Holt, P. D.; Reid, R. R.; Lewis, B. L.; Luther, G. W., III; Butler, A. *Inorg. Chem.* **2005**, *44*, 7671−7677.

(5) Zhang, G.; Amin, S. A.; Kupper, F. C.; Holt, P. D.; Carrano, C. J.; Butler, A. *Inorg. Chem.* **2009**, *48*, 11466−11473.

(6) Amin, S. A.; Green, D. H.; Kupper, F. C.; Carrano, C. J. *Inorg. Chem.* **2009**, *48*, 11451−11458.

(7) Barbeau, K.; Rue, E. L.; Trick, C. G.; Bruland, K. W.; Butler, A. *Limnol. Oceanogr.* **2003**, *48*, 1069−1078.

(8) Barbeau, K.; Zhang, G.; Live, D. H.; Butler, A. *J. Am. Chem. Soc.* **2002**, *124*, 378−379.

(9) Barbeau, K.; Rue, E. L.; Bruland, K. W.; Butler, A. *Nature* **2001**, *413*, 409−413.

(10) Sayre, H.; Milos, K.; Goldcamp, M. J.; Schroll, C. A.; Krause, J. A.; Baldwin, M. J. *Inorg. Chem.* **2010**, *49*, 4433−4439.

(11) Rosell, F. I.; Mauk, A. G. *Coord. Chem. Rev.* **2011**, *255*, 737−756.

(12) Kennedy, D. P.; Incarvito, C. D.; Burdette, S. C. *Inorg. Chem.* **2010**, *49*, 916−923.

(13) Ciesienski, K. L.; Haas, K. L.; Dickens, M. G.; Tesema, Y. T.; Franz, K. J. *J. Am. Chem. Soc.* **2008**, *130*, 12246−12247.

(14) Ellis-Davies, G. C. R.; Kaplan, J. H. *Proc. Natl. Acad. Sci. U.S.A.* **1994**, *91*, 187−191.

(15) Bandara, H. M. D.; Kennedy, D. P.; Akin, E.; Incarvito, C. D.; Burdette, S. C. *Inorg. Chem.* **2009**, *48*, 8445−8455.
(16) Kaplan, J. H.; Ellis-Davies, G. C. R. *Proc. Natl. Acad. Sci. U.S.A.* **1988**, *85*, 6571−6575.
(17) Kupper, F. C.; Carrano, C. J.; Kuhn, J.-U.; Butler, A. *Inorg. Chem.* **2006**, *45*, 6028−6033.
(18) Martin, J. D.; Ito, Y.; Homann, V. V.; Haygood, M. G.; Butler, A. *J. Biol. Inorg. Chem.* **2006**, *11*, 633−641.
(19) Ito, Y.; Butler, A. *Limnol. Oceanogr.* **2005**, *50*, 1918−1923.
(20) Parker, C. A. *Proc. R. Soc. London, Ser. A* **1953**, 220.
(21) Nyhus, K. J.; Wilborn, A. T.; Jacobson, E. S. *Infect. Immun.* **1997**, 434−438.
(22) Abrahamson, H. B.; Rezvani, A. B.; Brushmiller, J. G. *Inorg. Chim. Acta* **1994**, *226*, 117−127.
(23) Shweky, I.; Bino, A.; Goldberg, D. P.; Lippard, S. J. *Inorg. Chem.* **1994**, *33*, 5161−5162.
(24) Chrisman, M. A.; Grabo, J. E.; Krause, J. A.; Baldwin, M. J., manuscript in preparation.
(25) Chandra, S. K.; Basu, P.; Ray, D.; Pal, S.; Chakravorty, A. *Inorg. Chem.* **1990**, *29*, 2423−2428.
(26) Plesch, G.; Kettmann, V.; Sivy, J.; Svajlenova, O.; Friebel, C. *Polyhedron* **1998**, *17*, 539−545.
(27) Glebov, E. M.; Pozdnyakov, I. P.; Grivin, V. P.; Plyusnin, V. F.; Zhang, X.; F. Wu, N. D. *Photochem. Photobiol. Sci.* **2011**, *10*, 425−430.

dx.doi.org/10.1021/ic500635q | *Inorg. Chem.* 2014, 53, 5781−5787